

Contents lists available at ScienceDirect

NeuroImage

journal homepage: www.elsevier.com/locate/neuroimage



Brief neuronal afterdischarges in the rat hippocampus lead to transient changes in oscillatory activity and to a very long-lasting decline in BOLD signals without inducing a hypoxic state



Alberto Arboit^a, Shih-Pi Ku^b, Karla Krautwald^a, Frank Angenstein^{a,b,c,d,*}

- a Functional Neuroimaging Group, Deutsches Zentrum für neurodegenerative Erkrankungen (DZNE), Leipzigerstr, 44, Magdeburg 39118, Germany
- ^b Department Functional Architecture of Memory, Leibniz Institute for Neurobiology (LIN), Magdeburg 39118, Germany
- ^c Center for Behavior and Brain Sciences (CBBS), Magdeburg, Germany
- ^d Medical Faculty, Otto von Guericke University, Magdeburg 39118, Germany

ARTICLE INFO

Keywords: Postictal state Negative BOLD 1H-NMR spectroscopy Gamma oscillations Electrophysiology

ABSTRACT

The effects of hippocampal neuronal afterdischarges (nAD) on hemodynamic parameters, such as blood-oxygenlevel-dependent (BOLD) signals) and local cerebral blood volume (CBV) changes, as well as neuronal activity and metabolic parameters in the dentate gyrus, was investigated in rats by combining in vivo electrophysiology with functional magnetic resonance imaging (fMRI) or ¹H-nuclear magnetic resonance spectroscopy (¹H-NMRS). Brief electrical high-frequency pulse-burst stimulation of the right perforant pathway triggered nAD, a seizurelike activity, in the right dentate gyrus with a high incidence, a phenomenon that in turn caused a sustained decrease in BOLD signals for more than 30 min. The decrease was associated with a reduction in CBV but not with signs of hypoxic metabolism. nAD also triggered transient changes mainly in the low gamma frequency band that recovered within 20 min, so that the longer-lasting altered hemodynamics reflected a switch in blood supply rather than transient changes in ongoing neuronal activity. Even in the presence of reduced baseline BOLD signals, neurovascular coupling mechanisms remained intact, making long-lasting vasospasm unlikely. Subsequently generated nAD did not further alter the baseline BOLD signals. Similarly, nAD did not alter baseline BOLD signals when acetaminophen was previously administered, because acetaminophen alone had already caused a similar decrease in baseline BOLD signals as observed after the first nAD. Thus, at least two different blood supply states exist for the hippocampus, one low and one high, with both states allowing similar neuronal activity. Both acetaminophen and nAD switch from the high to the low blood supply state. As a result, the hemodynamic response function to an identical stimulus differed after nAD or acetaminophen, although the triggered neuronal activity was similar.

1. Introduction

Seizure activity is usually a self-limiting event—that is, in most cases it is terminated by an intrinsic mechanism that becomes effective during periods of heavy synchronous electrical discharges. Although seizure activity (or an ictal phase) eventually ceases, neuronal activity remains affected by the previous strong activity, a period also known as the postictal state, before it eventually returns to normal activity (i.e., interictal phase). Mechanism(s) that stop heavy seizure activity as well as mechanisms that control and/or dominate the postictal state are still not well known, although an understanding of these mechanisms may lead to the development of new therapeutics to treat epilepsy (Berman, 2009; Bragin et al., 1997; Lado and Moshe, 2008). In particular, the postictal

state, which is usually longer than the corresponding seizure, is often accompanied by several symptoms, such as psychosis, confusion, cognitive defects, aphasia, and paresis. Thus, shortening this period would be beneficial for patients with epilepsy.

So far, it is difficult to identify the postictal state and to modify its characteristic mechanisms because there is no clear pathophysiological biomarker that could be used as a readout to check the efficacy of a specific intervention. Ideally, an approach is needed that induces with a high incidence a long-lasting postictal state (e.g., a procedure that induces seizure-like activity) and then monitors with high spatial and temporal resolution the transition from the ictal to the postictal state, the maintenance of the postictal state, and the transition to the interictal state/normal state.

E-mail address: frank.angenstein@dzne.de (F. Angenstein).

^{*} Corresponding author at: Functional Neuroimaging Group, Deutsches Zentrum für neurodegenerative Erkrankungen (DZNE), Leipzigerstr, 44, Magdeburg 39118, Germany.

Similarly to the work by Bragin and colleagues (Bragin et al., 1997), we observed in the hippocampus of rats the appearance of neuronal afterdischarges (nAD) when the right electrical perforant pathway was stimulated with short bursts of high-frequency pulses (Helbing et al., 2013). Because we performed electrical perforant pathway stimulation and in vivo field potential recordings in the right dentate gyrus during an fMRI experiment, we also measured blood-oxygen-level-dependent (BOLD) signals as an indirect marker for neuronal activity in the entire hippocampal formation. As expected, the presence of nAD, which normally last for about 10-15 s, coincided with an elevation in BOLD signals in the entire right hippocampus. However, when these fMRI experiments were analyzed without a conventional BOLD baseline correction algorithm, it turned out that after termination of nAD, the BOLD baseline signal rapidly declined and remained at a significantly lower level during all subsequent stimulation periods (Angenstein, 2019; Arboit et al., 2021; Bovet-Carmona et al., 2019). However, it remained open whether nAD or the repeatedly applied stimuli were responsible for this persistent decrease in baseline BOLD signals. If the sustained decline in baseline BOLD signals after termination of nAD actually reflects a postictal state of the hippocampus and can be utilized as an easily measurable marker for the presence of a postictal state, then the decline: (i) should always occur after nAD but not when the same stimulation did not trigger nAD; (ii) the signal decline should be longer lasting than the stimulus-related nAD; and (iii) the signal decline should be associated with an altered functional state of the hippocampus.

Recent work has already indicated that a period of strong seizure activity can cause severe and prolonged hypoperfusion/hypoxia (i.e., up to 80 min) in the hippocampus (Farrell et al., 2020, 2016). This phenomenon depends on a long-lasting elevation of calcium in vascular smooth muscle, and its sustained vasoconstriction (Tran et al., 2020). Because emerging hypoperfusion/hypoxia should also be reflected in reduced BOLD signals, we tested whether a single brief period of nAD was sufficient to cause a long-lasting decrease in hippocampal BOLD signals and whether this decrease was dependent on sustained vasoconstriction. In addition, we tested whether neurovascular coupling mechanisms remain effective during a prolonged modified vascular state (i.e., during sustained vasoconstriction). That is, we examined whether and how the efficacy of neurovascular coupling mechanisms changes after a brief period of nAD.

2. Material and methods

2.1. Animals

Animals were cared for and used according to a protocol approved by the Animal Experiment and Ethics Committee and in conformity with European conventions for the protection of vertebrate animals used for experimental purposes as well as institutional guidelines 86/609/CEE (November 24, 1986). The experiments were approved by the animal care committee of Saxony-Anhalt state (No. 42,502-2-1406 DZNE) and performed according to the Animal Research: Reporting In Vivo Experiments (ARRIVE) guidelines. Male Wistar Han rats (age 9-13 weeks) were housed individually under conditions of constant temperature (23 °C) and maintained on a controlled 12-h photoperiod. Food and tap water were provided ad libitum. A total of 97 rats were included in this study: 77 rats for BOLD measurements, 12 rats for CBV measurements, 13 rats for ¹H NMR measurements, and 5 rats for local field potential (LFP) recordings. Animals used for control conditions (i.e., without stimulation) were subsequently also used for stimulation experiments. There was at least 1 week between the two measurements.

2.2. Surgical procedure

Electrode implantation was performed as previously described in detail (Angenstein et al., 2007). Initial experiments confirmed that the

setup that was developed for use in a 4.7T animal scanner is also applicable for a 9.4T animal scanner. Briefly, for electrode implantation the rats were an esthetized with pentobarbital (40 mg/kg $_{\rm body\ weight},$ i.p.) and placed into a stereotactic frame. A bipolar stimulation electrode (114 µm in diameter, made from Teflon-coated tungsten wire, impedance 18-20 $K\Omega$) was placed into the perforant pathway in the right hemisphere at the coordinates AP: -7.4, ML: 4.1 mm from bregma, DV: 2.0 to 2.5 mm from the dural surface. A monopolar recording electrode (114 µm in diameter, made from Teflon-coated tungsten wire, impedance 18–20 $\mathrm{K}\Omega$) was lowered into the granular cell layer of the right dentate gyrus at the coordinates AP: -4.0 mm, ML: 2.3 mm from bregma, DV: 2.8 to 3.2 mm from the dural surface. Monosynaptic-evoked field potentials were measured during electrode implantation to control for the correct placement, especially with regard to electrode depth. Grounding and indifferent electrodes (silver wires) were set on the dura through the left side of the cranium, and fixed to the skull with dental cement and plastic screws. Following surgery, the animals were housed individually and given 1 week for recovery, with ad libitum food and water.

2.3. Combined fMRI and electrophysiological measurements

The experimental setup for simultaneous fMRI and electrophysiological measurements during electrophysiological stimulations of the right perforant pathway in a 9.4T animal scanner was adopted from the setup used in a 4.7T animal scanner. Animals were initially anesthetized with isoflurane (1.5-2%; in 50:50 N_2 : O_2 , v:v) and the anesthesia was switched to deep sedation by application of medetomidine (Dorbene, Pfizer GmbH, bolus: 50 $\mu g/kg$ body weight s.c. and after 15 min 100 $\mu g/kg$ body weight /h s.c.) after animals were fixed into the head holder and connected to recording and stimulation electrodes. Heating was provided from the ventral side. Body temperature was measured in some animals before and after the fMRI session; the temperature remained stable between 37.5 and 38.5 °C in all measured animals. The heart rate and breathing rate were monitored during the entire experiment using an MR-compatible monitoring and gating system for small animals (Model1030, SA Instruments, Inc. Stony Brooks, NY, USA); the breathing rate (between 40 and 60 breaths/min) and heart rate (between 220 and 300 bpm) varied between individual animals but remained stable in all individual animals during the fMRI measurement.

To stimulate the perforant pathway, bipolar pulses (pulse width 0.2 ms) at 50 μA (low intensity) or 350 μA (high intensity) were used. Low-intensity pulses elicited clear field excitatory postsynaptic potential (fEPSP) in the dentate gyrus without a population spike component, whereas high-intensity pulses elicited an fEPSP with a clear population spike component. A stimulation period consisted of eight bursts of 20 pulses, one burst at the beginning of each second. The 20 pulses were given at a frequency of 100 Hz, so that one burst lasted 200 ms. The electrophysiological responses were filtered with an antialiasing filter, that is, a low-pass filter (<1 Hz) and a high-pass filter (>5000 Hz) using an EX4-400 amplifier (Science Products, Hofheim, Germany), transformed by an analog-to-digital interface (power-CED, Cambridge Electronic Design, Cambridge, UK) and stored on a personal computer with a sampling rate of 13,000 Hz.

To test the effect of NMDA receptor modulators (MK801 as an antagonist [0.5 mg/kg $_{\rm body\ weight}$] or GLYX-13 [1 mg/kg $_{\rm body\ weight}$] as a positive modulator) or acetaminophen (250 mg/kg $_{\rm body\ weight}$) on stimulus-induced BOLD signal changes, these drugs were injected intraperitoneally 30 min before the first stimulation period (Fig. 1). To test the effect of acetaminophen (250 mg/kg $_{\rm body\ weight}$) on baseline BOLD signals, the drug was injected intraperitoneally 2 min after the onset of fMRI measurement (Fig. 1).

All fMRI experiments were performed on a 9.4T Bruker Biospec 94/20 scanner, equipped with a BGA12 HP (440 mT/m) gradient system. An 86 mm transmit/receive volume coil (Bruker Biospin MRI GmbH, Ettlingen, Germany) was used for radio frequency (RF) excitation, and a 20 mm planar surface coil (Bruker Biospin MRI GmbH)

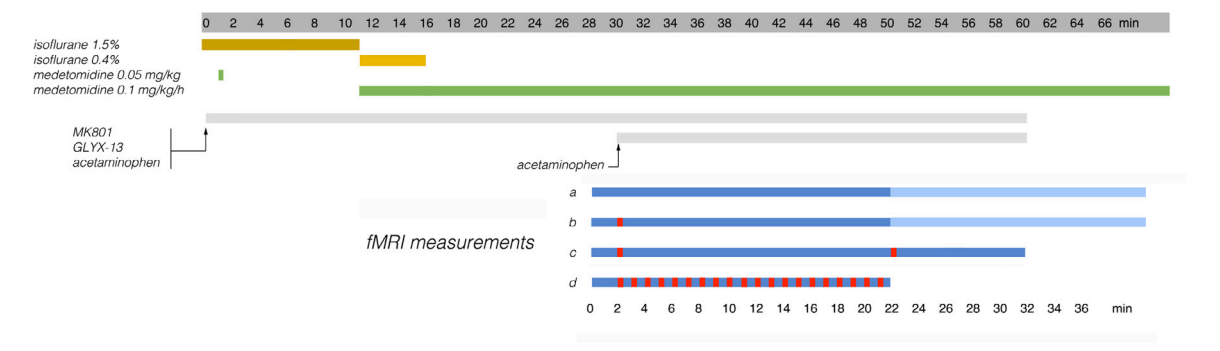


Fig. 1. Experimental design. In general, rats were first anesthetized with isoflurane (1.5–2%) and placed in the animal cradle, fixed in the head restraint, and connected to the recording and stimulation electrodes. Then, if mentioned, drug was injected intraperitoneally (time 0). After 1 min, a bolus of medetomidine (50 μg/kg body weight) was administered subcutaneously, and the animal was placed in the scanner to make all necessary preliminary settings for fMRI measurement. Ten minutes later, isoflurane was reduced to 0.4%, and continuous subcutaneous injection of medetomidine (100 μg/kg body weight /h) was started. Five minutes later, isoflurane was completely discontinued. fMRI started 28 min after drug application, so that the first stimulation period started 30 min after drug application. Basically, four different protocols were used: a, without any stimulation; b, with one stimulation period; c, two stimulation periods at an interval of 20 min; or d, repeated stimulation with an interval of 1 min. The measurement duration was 22 min (a, b, d) or 32 min (c). For the measurement of long-term effects, the measurement time was also extended to 2 h (a,b). Stimulation periods are indicated in red (For interpretation of the references to color in this figure legend, the reader is referred to the web version of this article.).

was used for signal reception. Initially, a B0-field map was acquired, which was used for local shimming using an ellipsoid that covered the entire brain. BOLD-fMRI was performed by using a gradient-echo planar imaging (EPI) sequence with the following parameters: TR 2000 ms, TE 20.61 ms, flip angle 90°, bandwidth 326,087 Hz, slice number: 10, slice thickness 0.4 mm, inter slice distance 0.1 mm, field of view (FOV) 25.6×25.6 mm, matrix 128×128 (in plane resolution 200×200 µm).

Trigger pulses that were generated by the scanner at the beginning of every volume—that is, every 2 s—were used to synchronize fMRI image acquisition and electrophysiological stimulations. Electrical stimulation started with a delay of 175 ms to prevent an overlay of electrophysiological responses with scanner-induced artifacts (Fig. 2). Each fMRI measurement started with an initial 2-min period without any stimulation (to determine baseline BOLD signals), and then the appropriate stimulation protocol was applied. Changes in CBV were measured with identical imaging parameters but 5 min after i.v. injection (through the tail vein) of 20 mg/kg body weight ultrasmall superparamagnetic iron-oxide (USPIO) nanoparticles (Molday ION, BioPAL Inc., Worcester, MA, USA). The concentration of 20 mg/kg $_{body\ weight}$ USPIO was used because it is close to the optimal contrast-to-noise ratio and has a low (calculated) BOLD contribution to the CBV-weighted MRI (Lu et al., 2007). Because the presence of USPIO reduces fMRI signal intensities, an increase in CBV is indicated by a decrease in fMRI signals.

After fMRI measurements, 10 horizontal anatomical spin-echoimages (T_2 -weighted) were obtained using a rapid acquisition relaxation enhanced (RARE) sequence (Hennig et al., 1986) with the following parameters: TR 3000 ms, TE 33 ms, slice thickness 0.4 mm, FOV 25.6 \times 25.6 mm, matrix 256 \times 256, RARE factor 8, averages 4. The total scanning time was 6.4 min. The slice geometry, 10 horizontal slices, was identical to the previously obtained gradient-echo EPI.

2.4. Combined $^1{\rm H}$ NMR spectroscopy and electrophysiological measurements

To avoid putative interferences with the implanted electrodes, the left dorsal hippocampus was used for 1H NMR spectroscopy. First, three adjacent localizer anatomical T1-weighted images were obtained in three orthogonal planes to align a rectangular voxel volume (2 \times 2 \times 4 mm) in the left dorsal hippocampus. Then, first and second order shims were performed for the defined voxel using the localized shim tool implemented in ParaVision 6.0. A point resolved spectroscopy sequence (PRESS) with the following parameters was used to obtain to a 1H NMR spectrum: TR 3000 ms, TE 16.301 ms, acquisition dura-

tion 511.18 ms, bandwidth 8012.82 Hz (20.02 ppm), dwell time 62.4 μs, spectral resolution 0.98 Hz/pts, averages 300; the result was a total scanning time of 15 min. The PRESS sequence was preceded by a variable pulse power and optimized relaxation delays (VAPOR) sequence for global water suppression. All raw spectra were analyzed with the freely available LCModel software (http://s-provencher.com/lcmodel.shtml) (Provencher, 1993) using the basis set of LCModel model metabolite spectra for 9.4T (http://s-provencher.com/lcm-basis.shtml). The unsuppressed water signal measured from the same VOI was used as an internal reference for the quantification (assuming 80% brain water content). CRLB (Cramér Rao Lower Bounds) value greater than 50% was used to exclude lines from the analysis. In addition, the ratio of each metabolite to total creatine (i.e., creatine and phosphocreatine) was determined to evaluate possible changes in concentration after stimulation, assuming that the total creatine concentration did not change as a result of stimulation. In the analysis, possible BOLD effects on the line width of individual metabolites due to changes in oxygenated Hb in the hippocampus after stimulation were not considered separately, because according to LCModel the rough estimate of linewidth in the in vivo spectrum before (FWHM before: 0.050 ± 0.019 ppm) and after a stimulation train $(0.0512 \pm 0.015 \text{ ppm})$ did not differ significantly.

2.5. LFP recordings

We also recorded LFP outside the scanner to monitor ongoing neuronal activity in the dentate gyrus during and after stimulation. Signals were filtered (high-pass filter: 0.1 Hz; low-pass filter: 5000 Hz) using EX1 amplifiers (Science Products, Hofheim, Germany) and transformed by an analog-to-digital interface (power-CED, Cambridge Electronic Design). Data were recorded by using a sampling rate of 5000 Hz with Spike2 (version 6).

2.6. Data analysis

The functional data were loaded and converted to the BrainVoyager data format. A standard sequence of pre-processing steps implemented in the BrainVoyager QX 2.8.0 software (Brain Innovation, Maastricht, the Netherlands) such as slice scan time correction, 3D motion correction (trilinear interpolation and data reduction by using the first volume as a reference), and temporal filtering (FWHM 3 data points) were applied to each data set.

VOI analysis: Each individual functional imaging data set was aligned to a 3D standard rat brain by using the 3D volume tool implemented

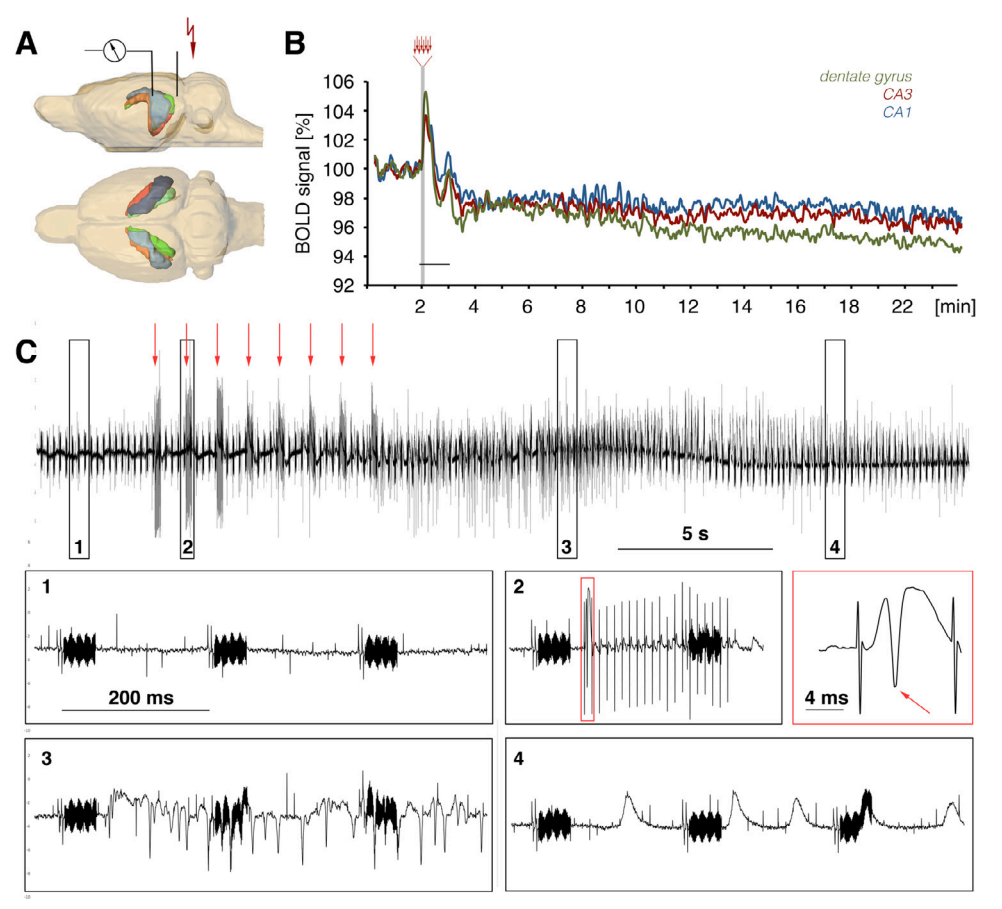


Fig. 2. Experimental setup to simultaneously monitor electrophysiological and BOLD-fMRI responses in the in rat brain during electrical perforant pathway stimulation. A Schematic view of electrode locations and analyzed VOIs (green: dentate gyrus; red: CA3; blue: CA1). B Example of a BOLD time series measured in individual VOIs during one fMRI experiment. A gray vertical bar indicates the period of stimulation and the black horizontal bar indicates the time period of nAD. C Example of an electrophysiological recording during an fMRI measurement. Top: Summary of 30-s-long recording period. Red arrows indicate the periods of stimulation (i.e., eight bursts of 20 highfrequency pulses). Bottom: Compilation of electrophysiological recordings with higher temporal resolution. 1, Before electrical stimulation started, only scanner-related artifacts were observed. 2, During each pulse burst stimulation, only one population spike as a response to the first pulse was observed (magnified to the right side). 3, Immediately after stimulation, heavy spiking-an appearance of frequent population spikes—was observed. 4, When heavy spiking abated, then large fEPSP-like responses appear (For interpretation of the references to color in this figure legend, the reader is referred to the web version of this article.).

in the BrainVoyager QX 2.8.0 software. The 3D standard rat brain had previously been generated from a rat of the same age and strain. The following VOIs were marked in the 3D standard rat brain: CA1, CA3, dentate gyrus, septum, and medial prefrontal cortex (mPFC). The averaged BOLD time series of all voxels located in one VOI was then calculated for each individual animal using the VOI analysis tool implemented in the BrainVoyager QX 2.8.0 software. Each individual BOLD time series was normalized by using the averaged BOLD signal intensity of 100%. Normalized BOLD time series were then averaged and are depicted as mean BOLD time series \pm SEM.

Analysis of LFP recordings: We measured the amplitude of the population spike in mV, the latency in ms, and the slope in mV/ms (measured at the steepest rise of the first negative deflection). To visualize how these parameters were affected by different stimulation protocols or pharmacological stimulation, we averaged the responses in one train and compared them between two conditions (i.e., comparison of stimulation train 1 control vs. drug [e.g., acetaminophen] or comparison of train 1 vs. train 2 in the same animal) using a Student's unpaired t-test. We considered differences to be significant when p < 0.05. All absolute measurements were averaged and are presented as the arithmetic mean \pm SEM.

The frequency band-specific power from the LFP recordings was estimated from the Hilbert transform of frequency band-filtered LFP recordings. This approach has been termed "clinical mode decomposition" (Cohen et al., 2008; Freeman, 2004), and it is useful to inspect the changes in oscillatory dynamics in specific frequency bands. This analysis was performed by using custom codes in Spyder 4.2.5 (Python 3.8.8). The data were band-pass filtered using the following ranges: delta (1–4 Hz), theta (4–8 Hz), alpha (8–13 Hz), beta (13–30 Hz), low gamma (30–49 Hz), middle gamma (51–90 Hz), fast gamma (90–140 Hz), and ultra-high gamma (140–170 Hz). The ranges were chosen to remove the

50 Hz line noise. Before band filtering the data were down-sampled to 1000 Hz. Finite pulse response (FIR) filters were used to have no distortion or changes in phase that can happen when infinite pulse response (IIR) filters are used. The Hilbert transform was then applied to the filtered data, and the instantaneous power at each time point was obtained by calculating the absolute value of the Hilbert transform raised to the second power. After extracting the power, to quantify the power changes over time of the filtered frequency bands, three intervals were chosen to analyze the power: (i) a baseline period starting 150 s before the stimulation, (ii) an interval 350 s after the stimulation, and (iii) an interval 900 s after the stimulation. Each interval lasted 120 s. The power of each frequency band was then normalized to the baseline using the percentage change method (% change = $100 \times [(signal - baseline)/baseline])$. In this way, it was possible to average together the normalized power of all animals. For each frequency band, changes in normalized power between the selected intervals (i, ii, and iii) were tested by using either a one-way ANOVA or the Kruskal-Wallis test, depending on the homogeneity of variance (tested by using the Brown-Forsythe test). For multiple comparisons, Tukey's and Dunn's post hoc tests were performed depending on the requirements. Differences were considered significant when p < 0.05. Unless stated otherwise, data are expressed as the mean ± SEM (standard error mean). To better visualize the time course of the normalized power of the selected frequency bands, a smoothing window of 20 s was applied to the normalized data prior to plotting. All spectrograms were calculated by using the specgram function from matplotlib in Spyder 4.2.5 (Python 3.8.8) with a Hanning window of 1 s and an overlap of 0.5 s.

Analysis of pulse-related neuronal activity recorded during fMRI: Spiking and postsynaptic activity of granule cells in the dentate gyrus were analyzed as described previously (Angenstein, 2019). Briefly, the amplitude of the population spike was measured in mV (from the first most

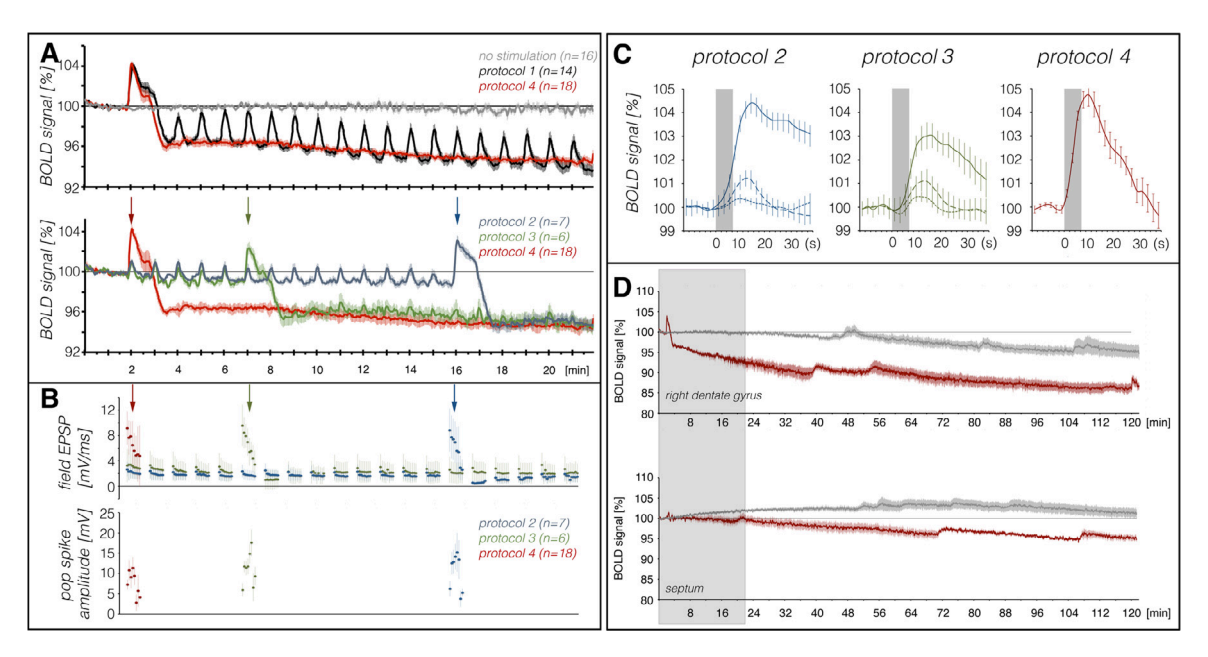


Fig. 3. Variation in BOLD signals and electrophysiologically measured neuronal responses in the right dentate gyrus during stimulation of the right perforant pathway with four different stimulation protocols. A Summary of BOLD signal changes in the right dentate gyrus during each stimulation condition. Protocol 1 consisted of 20 identical high-intensity pulse burst stimulations (black line, top panel). Protocol 2 (blue line, lower panel) and protocol 3 (green line) used repetitive low intensity pulse (50 µA) trains that were substituted by one high-intensity pulse train (protocol 2: train 15, indicated by a blue arrow; protocol 3 train 5, indicated by a green arrow). Protocol 4 used only one high-intensity pulse bust train 2 min after the start of the fMRI measurement (red arrow). The gray graph indicates the variation in BOLD signals when the perforant pathway was not stimulated. Note that all four stimulation protocols resulted in a similar decline in baseline BOLD signals at the end of the measurement after 22 min. B Summary of concurrently measured neuronal responses in the right dentate gyrus during stimulation. High-intensity pulse bursts only elicited detectable population spikes, which were accompanied by stronger postsynaptic responses (measured as the initial slope of the fEPSP). In contrast to BOLD responses, postsynaptic responses to low-intensity pulse burst stimulation did not differ between initial (i.e., before high-intensity pulse burst stimulation) and late (i.e., after high-intensity pulse burst stimulation) stimulation trains. C Summary of BOLD responses induced before the high-intensity pulse burst stimulation (average of trains 1-5, dashed lines), during the high-intensity pulse burst stimulation (solid line) and after the high-intensity pulse burst stimulation (average of trains 16-20, dotted lines). D Development of BOLD signals in the right dentate gyrus and septum over the course of 2 h after stimulation. When a single stimulation period induced nAD, then BOLD signals declined and remained significantly reduced compared with the BOLD signals in animals that were not stimulated (gray line). Note that in unstimulated animals, baseline BOLD signals remained constant for about 45 min; thus, all subsequent experiments did not exceed 30 min. The dark gray box indicates the time period that was used for the initial experiments depicted in A (For interpretation of the references to color in this figure legend, the reader is referred to the web version of this article.).

positive point to the following most negative point) and the latency in ms (from the middle of the stimulus artifact to the most negative point; see Fig. 2C). Postsynaptic activity was measured as the initial slope of the fEPSP (mV/ms). All absolute measurements were averaged and are depicted as the arithmetic mean \pm SEM.

3. Results

Repetitive stimulations of the right perforant pathway with bursts of high-frequency pulses caused, as described previously (Angenstein, 2019), transient positive BOLD responses as well as a sustained decrease in baseline BOLD signals in the right and left hippocampus.

In the present study, we used four different stimulation protocols to investigate whether and how the occurrence of nAD affected BOLD signals. In these protocols, the perforant pathway was stimulated either with high-intensity repetitive pulse trains (protocol 1), with one high-intensity pulse train in combination with low-intensity repetitive pulse trains (protocols 2 and 3), or with a high-intensity pulse train only (protocol 4; Fig. 3A,B). When the perforant pathway was stimulated with repeated high-intensity pulse burst periods (protocol 1), nAD were observed only during and after the first stimulation period and did not occur during any subsequent stimulation period. After the second stimulation period, baseline BOLD signals declined below the initial level and remained there until the end of the experiment (black line, Fig. 3A). Superimposing BOLD time series from different hippocampal subregions revealed that both transient positive BOLD responses and the concurrent

persistent decline in baseline BOLD signals were characteristic for all analyzed hippocampal subregions, and they were significantly stronger in the right dentate gyrus compared with the right CA1 and CA3 regions. By contrast, BOLD time series from the left dentate gyrus, CA1, and CA3 were similar, with only small differences in transient positive BOLD responses but no significant differences in the development of baseline BOLD signals (Fig. S1).

3.1. Development of baseline BOLD signals during low- and high-intensity pulse stimulations

To exclude possible scanner-, electrode-, analyzer-, or sedation-related (i.e., medetomidine) artifacts on the development of the base-line BOLD signal, we then measured animals that were connected to the electrophysiological setup but did not receive electrical stimulation. Under this condition, baseline BOLD signals in all hippocampal subfields remained stable over a 22 min period, so we did not detect any confounding factors on baseline BOLD signals (gray line, Fig. 3A).

In the next series of experiments, we tested whether repeated activation of granule cells (i.e., repetitive synaptic and/or spiking activity) was required to maintain the long-lasting reduction in baseline BOLD signals. First, the perforant pathway was again stimulated with repetitive trains of high-frequency pulses but with low intensities (50 μ A)—that is, pulse intensities that triggered only fEPSP but not population spikes (Fig. S2) or nAD in the dentate gyrus (protocol 2). Baseline BOLD signals declined by about 1% in the right dentate gyrus (blue line, Fig. 3A). However, when the same pulse sequence was given once at a high in-

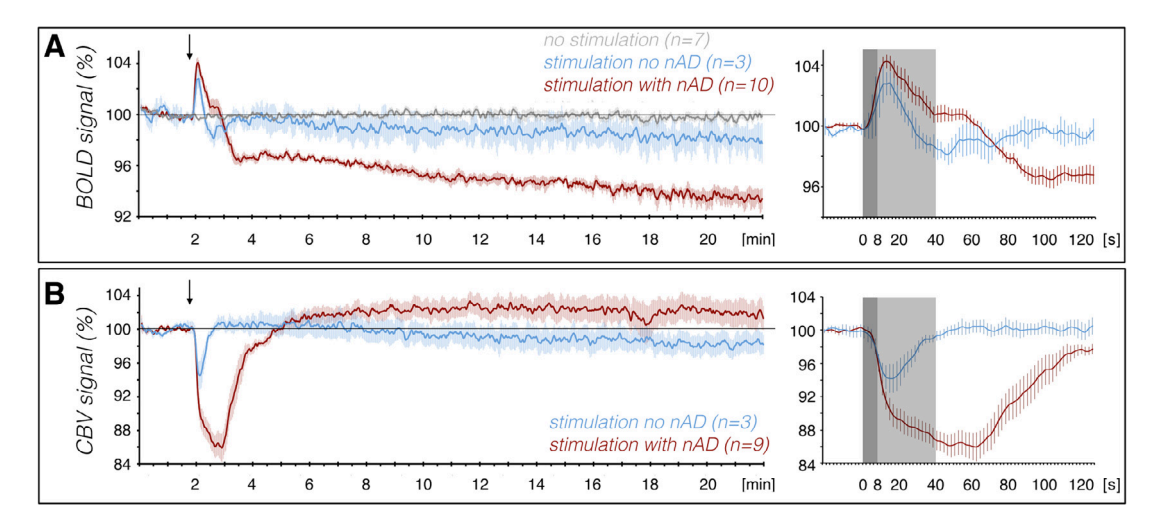


Fig. 4. Variation in BOLD (A) and CBV (B) signals after one stimulation period that elicited nAD (red lines) or did not elicit nAD (blue lines). The black arrow indicates the onset of stimulation. Right side: Detail of signal variations during and immediately after stimulation. The dark gray box indicates the time period of electrical stimulation, and the light gray box indicate the time period of nAD (For interpretation of the references to color in this figure legend, the reader is referred to the web version of this article.).

tensity (350 μ A), population spikes and nAD were induced, and subsequently the baseline BOLD signals decreased to a much lower level—to approximately 95%—and remained at this low level until the end of the experiment.

Subsequently applied low intensity pulses did not further affect baseline BOLD signals; they only generated attenuated positive BOLD responses. To confirm that stimulus-induced positive BOLD responses were reduced after baseline BOLD signals declined, we repeated the same experiment but applied the high-intensity stimulation train after five low-intensity stimulation trains (protocol 3). Again, baseline BOLD signals only dropped after the single high-intensity stimulation train, and all subsequent stimulus-related positive BOLD responses were significantly reduced compared with the initial response (green line, Fig. 3A). In contrast to the altered BOLD responses, the initial slopes of the fEPSPs in the dentate gyrus, as a measure of postsynaptic activity, remained unchanged (Fig. 3B).

3.2. nAD but not pulse-related neuronal responses caused the decline in baseline BOLD signals

To test whether the sustained decrease in baseline BOLD signals is maintained by repeated low-intensity stimulations, that is, repeated synaptic activations, the right perforant pathway was stimulated with only one stimulation period, namely eight high-intensity pulse bursts (protocol 4; red line, Fig. 3A). This stimulation protocol triggered nAD in 18 out of 22 animals; thus, in four animals BOLD signal changes only depended on neuronal activity induced by electrical stimulations and not on nAD. During the stimulation period, BOLD signals rapidly increased and reached a maximum level 2 s after the stimulation ceased. When nAD were subsequently generated, then BOLD signals declined slowly but remained elevated compared with the initial level (red line, Figs. 3A and 4A), whereas in the absence of nAD, BOLD signals rapidly returned to the initial level (blue line, Fig. 4A). After nAD terminated, BOLD signals remained at a short stable level before they eventually declined to a low level, where they remained for the next 20 min, although no further stimulations were applied (Figs. 3A and 4A). When no nAD were induced, no significant decline in baseline BOLD signals was observed. Thus, the clear sustained decline in baseline BOLD signals required the presences of nAD.

All four stimulation protocols tested resulted in similar levels of baseline BOLD signals at the end of the experiment: It did not matter whether and when additional low- or high-intensity pulse trains were given. Thus, a short period of nAD caused the prolonged decline in baseline BOLD signals.

In an additional set of experiments, we tested whether the nADmediated decrease in baseline BOLD signals returned to normal within the following 2 h. Once nAD caused a decrease in baseline BOLD signals, they remained at the low level; even within 2 h, the initial BOLD baseline value was not regained (Fig. 3D). In animals connected to the electrophysiological setup but that did not receive an electrical stimulation, baseline BOLD signals remained stable for about 40 min and then gradually declined by up to 5% until the end of the measurement. Similarly to a previous observation (Shatillo et al., 2019), there were occasional spontaneous BOLD waves that did not relate to detectable changes in synchronized neuronal activity in the dentate gyrus. These spontaneous BOLD waves occurred in both stimulated and unstimulated animals, in the hippocampus, and at other time points in the prefrontal cortex; thus, they do not represent general scannerrelated artifacts (Fig. S3). Because the baseline BOLD level in the dentate gyrus remained stable for 40 min, we focused on the development of BOLD signals during the first 30 min after stimulation in all subsequent studies to avoid confounding factors that might become effective after 40 min.

3.3. Stimulus-related change in the local CBV

After testing the four different stimulation protocols, it became obvious that the presence of nAD was responsible for the prolonged decline in baseline BOLD signals. For this reason, we performed further experiments with stimulation protocol 4, because with this protocol nAD were triggered with only one stimulation period. A decline in BOLD signals indicates reduced oxygenation of capillary/venous blood, which in turn could be the result of higher oxygen consumption in the surrounding tissue, a reduced blood supply, or a combination of these two parameters. To measure putative stimulus-related changes in local blood volume, we reran the same experiment in the presence of 20 mg/kg body weight USPIO. As expected, a single stimulation period caused a fast decline in signal intensities: a fast increase in blood volume in the right and left dorsal hippocampus (red line, Fig. 4B). In contrast to the development of BOLD signals, CBV remained at this high level during the subsequent period of nAD; thus, the maximum CBV was still present during nAD. CBV then declined to near the initial level, and after approximately 2 min, it declined below the initial level and remained at that reduced level until the end of the measurement. When stimulation did not trigger nAD,

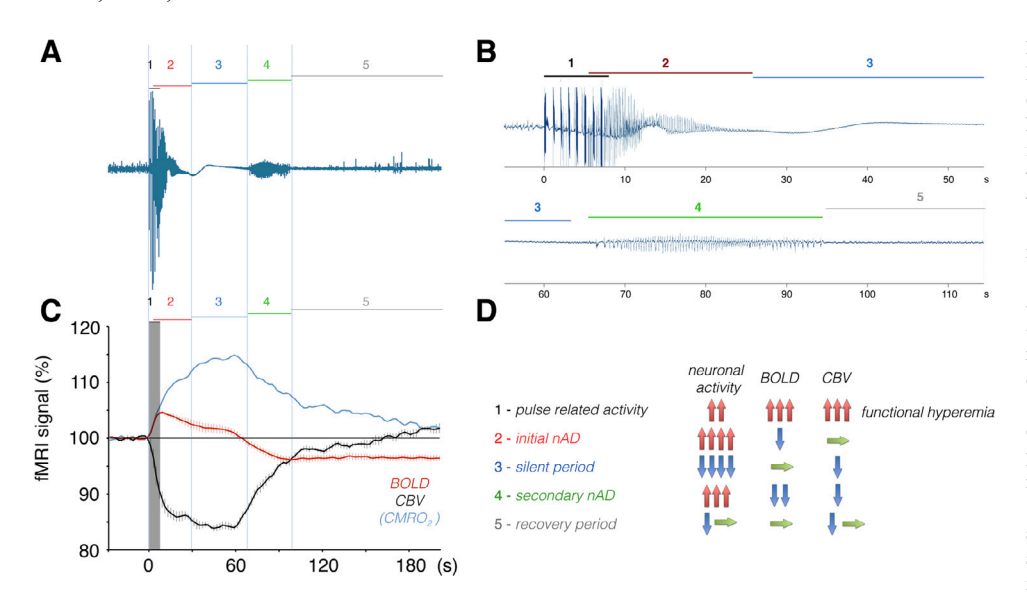


Fig. 5. Temporal comparison of electrophysiological and hemodynamic responses in the right dentate gyrus during and immediately after high-frequency pulse burst stimulation. A During electrical stimulation of the perforant pathway, neuronal responses to electrical pulses as well as initial discharges were observed (phase 1). Already after the sixth pulse burst, clear nAD were triggered, which lasted for about 15 s (phase 2). After termination of nAD, neuronal activity almost completely collapsed for about 40 s (phase 3). C After a period of almost no neuronal activity, another period of nAD occurred, again ending after approximately 25 s (phase 4). Thereupon, neuronal activity apparently returned to normal (phase 5). B An example of an electrophysiological recording of neuronal activity with higher temporal resolution (phases 1-5 correspond to the time periods described in A). C Comparison of BOLD and CBV signal changes and CMRO2 values calculated from them at different phases of neuronal ac-

tivity. BOLD and CBV signals correspond to Fig. 3, and CMRO₂ has been roughly estimated by calculating -CBV_{signal} - BOLD_{signal}. D Summary of changes in neuronal activity, BOLD, and CBV signals during each phase. Only phase 1 showed clear functional hyperemia, that is, after an increase in neuronal activity, blood flow/volume increased, which in turn was accompanied by a larger BOLD signal.

then CBV only increased transiently and returned quickly to the initial level (blue line, Fig. 4B).

3.4. nAD-related changes in ongoing neuronal activity in the dentate gyrus

During fMRI, scanner-related artifacts (i.e., switching gradients) confound the in vivo recordings. Although pulse-induced synchronized granule cell activity could easily be detected and quantified, small changes in LFP signals, as a measure of ongoing baseline neuronal activity, were superimposed by scanner-induced interferences. Therefore, outside the MRI scanner, we measured the development of LFPs during and after a single stimulation period (Fig. 5). Before stimulation, ongoing synchronized neuronal activity was stable (Figs. 5 and 6A,B). Already during the stimulation period heavy neuronal activity emerged and continued for about 15-20 s. This increase in neuronal activity was not uniform—it changed over time. Initially, strong synchronized spiking activity was observed, which was then replaced by neuronal activity triggering fEPSP-like responses (Figs. 2 and 5). After nAD terminated, neuronal activity almost completely disappeared for the following 30-40 s. Then, a second period of increased neuronal activity occurred, lasting approximately 20-30 s. When this second period of increased neuronal activity terminated, neuronal activity slowly recovered during the next 5 min to an activity pattern seen before stimulation onset (Figs. 5 and 6A,B).

Although total neuronal activity apparently normalized after 4–5 min, frequency band analysis revealed a transient significant increase in low gamma oscillations (30–49 Hz) after 6 min, whereas theta oscillations (4–8 Hz) and to a lesser extend alpha oscillations (8–13 Hz) only slowly recovered and were still significantly reduced at this time point (Fig. 6C,D). All other frequency bands returned to baseline within 6 min after the end of stimulation (Fig. S4).

3.5. Relation between neuronal activity CBV and BOLD signals

A single 8-s-long period of high-frequency pulse burst stimulation elicited various forms of neuronal activity in the dentate gyrus that outlasted the stimulation period by approximately 15 min (Fig. 6). In contrast to neuronal activity, hemodynamic parameters remained changed for at least 30 min (Fig. 3D). To address what kind of neuronal activity relates to changes in CBV and BOLD signals, we overlayed the measured hemodynamic parameters with measured neuronal activity in the dentate gyrus (Figs. 5 and 6). During stimulation, pulse-induced granule

cell responses caused a clear functional hyperemia, with increased CBV and BOLD signals (blood oxygenation) after a short delay (Fig. 5, period 1). During the subsequent period of nAD (Fig. 5, period 2), CBV further increased, whereas BOLD signals declined, indicating that tissue oxygen consumption further increased. After nAD terminated, almost no neuronal activity was detected for about 30-40 s, and during this time the BOLD signal stabilized, while CBV remained at the highest level and started to decline only at the end (Fig. 5, period 3). The subsequent second period of nAD, which lasted again for 20-30 s, coincided with a strong decline in CBV toward the initial level, and BOLD signals declined below the initial level (Fig. 5, period 4). Then, neuronal activity slowly recovered to an apparent similar level as present before the stimulation (Figs. 5 and 6, period 5). During this period, BOLD signals remained at the low level and CBV decreased below the initial level. When CBV and BOLD signals were used to roughly calculate tissue oxygen consumption (i.e., BOLD-CBV), at the end of period 5 oxygen consumption returned to a level that was present before stimulation and remained stable for the next 14 min (Fig. 6E,F). During the subsequent period of increased low gamma-oscillatory activity (Fig. 6D, period 6), CBV continued to decrease only slowly. At the end of period 6, CBV reached an apparently stable level. Although a transient increase in low gamma oscillation was present, the BOLD signals remained unaffected (Fig. 6F).

3.6. NMDA receptor activation and baseline BOLD signals

The baseline BOLD signal only persistently declined by more than 5% when stimulation intensities were high enough to elicit population spikes and nAD in the hippocampus. To test whether postsynaptic NMDA receptors are involved in this phenomenon, we stimulated the right perforant pathway again with a high-intensity stimulation train but in the presence of MK801, a systemically acting NMDA receptor antagonist. The presence of 0.5 mg/kg body weight MK801 did not completely block the appearance of nAD: They were again elicited in five out of eight animals. The initial transient positive BOLD response was similar in the two groups treated with MK801, and BOLD signals only significantly declined below the initial level in animals that had nAD. Thus, the presence of nAD was again essential for the subsequent decline in baseline BOLD signals (Fig. 7A). Comparing the group of MK801-treated animals that showed nAD with untreated animals (that also had nAD) revealed an effect of MK801 on the development of BOLD signals during the experiment. First, the initial transient positive BOLD response was sig-

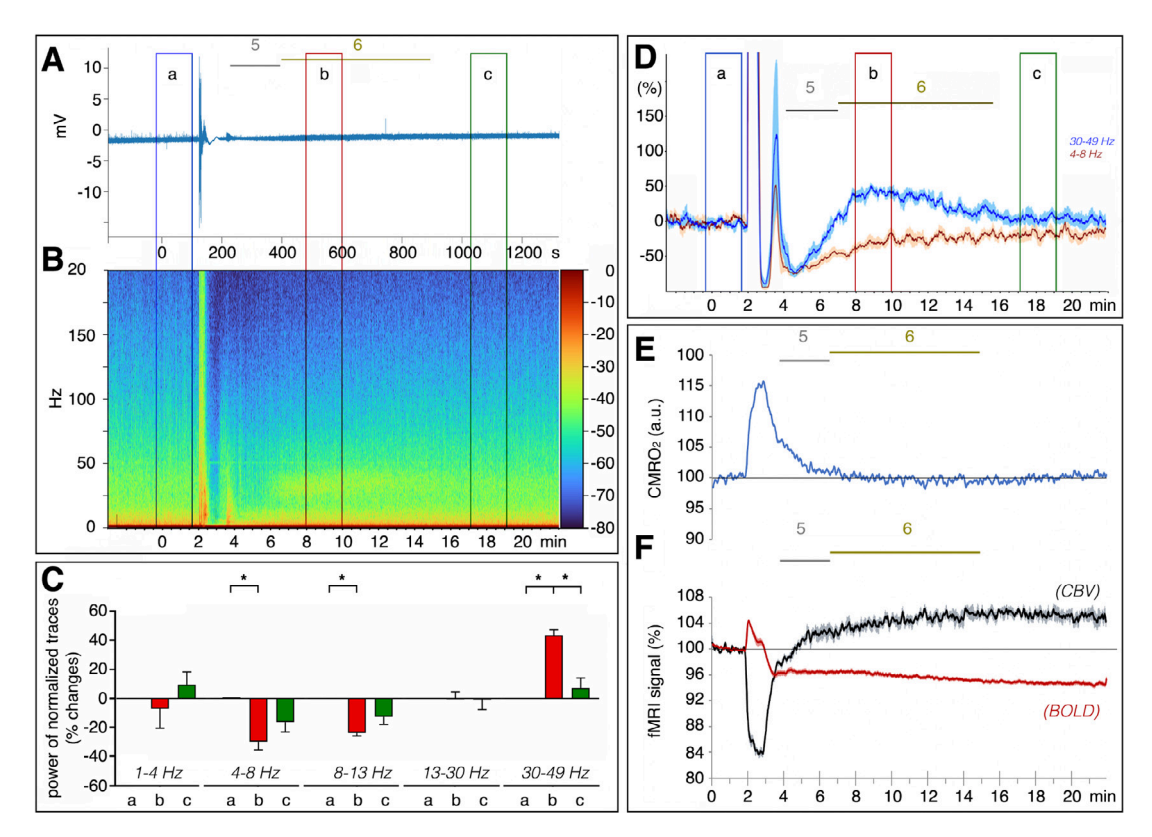


Fig. 6. Comparison of neuronal activity and hemodynamic responses in the right dentate gyrus during and after one high-frequency pulse burst stimulation. A Example of electrophysiological recordings in the dentate gyrus during a stimulation experiment with one stimulation period. B Example of a corresponding frequency spectrum of neuronal activity in the dentate gyrus. C Quantification of relative power of the low gamma (30–49 Hz) and theta (4–8 Hz) frequency bands at three different time points: a, before stimulation (blue box in C-E); b, 350 s (red box in C-E) after stimulation; and c, 900 s after stimulation (green box in C-E). The asterisk indicates significant differences (Dunn's post hoc tests, p < 0.05, n = 5). D Corresponding development of ongoing neuronal activity in the stimulated right dentate gyrus shown as the averaged power spectrum of low gamma (blue lines) and theta (red lines) oscillatory activity. After cessation of secondary nAD, that is, during the period when total neuronal activity and CMRO₂ appeared to normalize (phase 5, see also Fig. 4), low-level gamma oscillatory activity temporarily increased for about 8 min (*phase* 6). By contrast, theta oscillatory activity recovered only slowly and uniformly after the second period of nAD (n = 5). Peak value for the 4–8 Hz band: 2073.52 \pm 548.12 and for the 30–49 Hz band: 3034.66 \pm 488.06. E Estimation of corresponding changes in CMRO₂ in the dentate gyrus (blue line) during a stimulation trial with one stimulation period. F CMRO₂ was calculated from the BOLD (red line) and CBV (black line) time series in the dentate gyrus (CMRO₂ = -CBV signal - BOLD signal) (For interpretation of the references to color in this figure legend, the reader is referred to the web version of this article.).

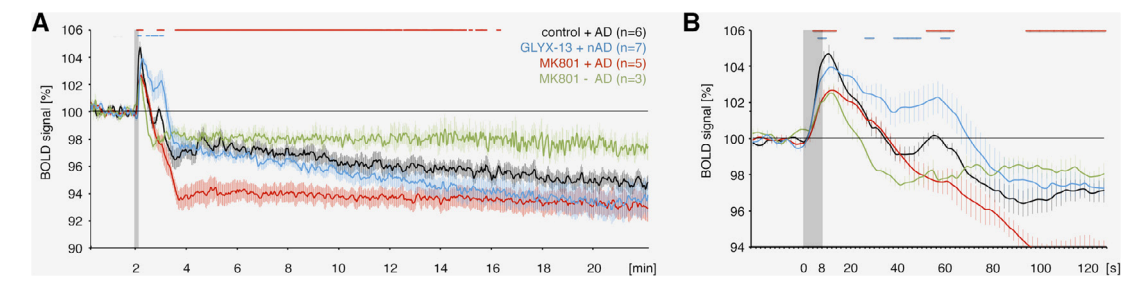


Fig. 7. Modulation of NMDA receptors had only minor effects on baseline BOLD signals after nAD. A BOLD time series in the right dentate gyrus after stimulation of the right perforant pathway in the presence of the NMDA receptor antagonist MK801 (red and green graphs) or the positive modulator GLYX-13 (blue graph). Note that the decline in baseline BOLD signals was similar after 20 min, although the initial decline was significantly altered. B Higher temporal resolution of BOLD signal changes immediately after nAD. The gray box indicates the period of stimulation. Periods with significant differences in BOLD signals (p< 0.05) between treated and untreated animals are indicated by a red (MK801 treatment) or blue (GLYX-13 treatment) marker line at the top (For interpretation of the references to color in this figure legend, the reader is referred to the web version of this article.).

nificantly smaller in MK801-treated animals compared with untreated animals (red line, Fig. 7A,B). Second, in MK801-treated animals, BOLD signals rapidly declined to a low level within 90 s after the end of stimulation and remained stable at this level for the next 20 min. By contrast, in untreated animals, after termination the BOLD signal decline was interrupted by a small plateau of increased neuronal activity and a slower decline in BOLD signals, so that the low level of baseline BOLD signals was only reached 15 min later (at the end of the experiment);

the reduced baseline BOLD level was the same in the MK801-treated and untreated animals (Fig. 7A). Thus, NMDA-receptor-mediated mechanisms only affected the BOLD signals during the period of nAD and the kinetics of the subsequent decline in BOLD signals, but not the strong decline in baseline BOLD signals at later time points.

To confirm that NMDA-receptor-dependent mechanisms were involved in the control of the initial development of baseline BOLD signals, we reran the same experiment in the presence of GLYX-13, a posi-

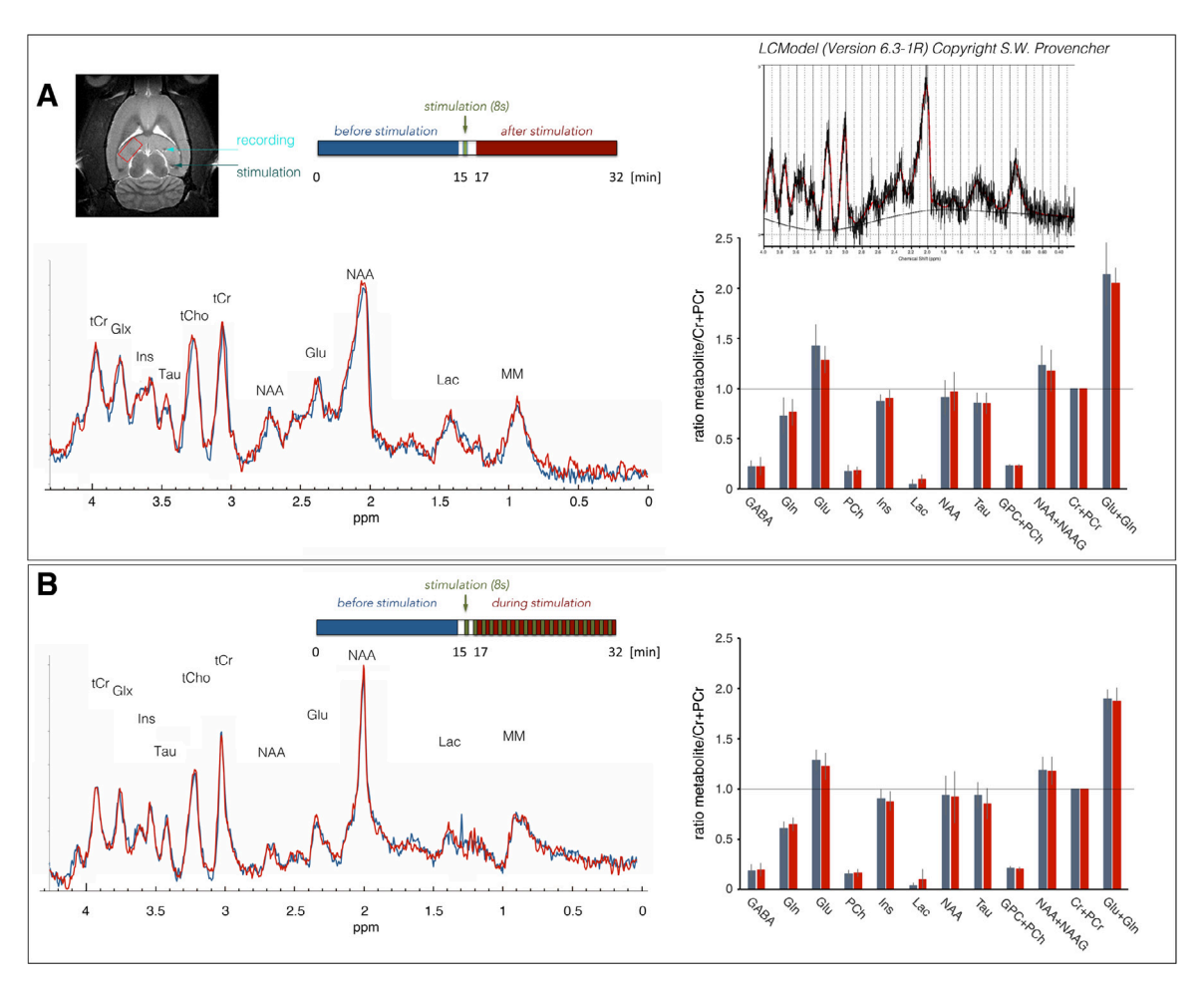


Fig. 8. Example of a 1 H NMR power spectrum in the left dorsal hippocampus (indicated by a red box) measured before (blue lines), after, and during stimulation (red lines) of the right perforant pathway. The perforant pathway was either stimulated with one period of high-frequency pulse bursts (A) or with repetitive periods of high-frequency pulse bursts (B). Relevant resonance signals for the metabolites quantified in our study are labeled; tCr, total creatine; Glx, glutamine and glutamate; Ins, inositol; Tau, taurine; tCho, choline; NAA, *N*-acetyl aspartate; Lac, lactate; MM, macromolecules. The chemical shift is expressed in parts per million (ppm). Right side: Individual metabolites were quantified using LCModel (insert at the top). All metabolite concentrations were related to total creatine concentration (i.e., creatine and phosphocreatine: Cr+PCr). Bars show the average of 6 (one stimulation period) or 7 (15 stimulation periods) animals \pm SD. The two stimulation conditions did not cause significant changes in the concentrations of the analyzed metabolites (For interpretation of the references to color in this figure legend, the reader is referred to the web version of this article.).

tive modulator of NMDA receptors. When GLYX-13 was present during stimulation of the right perforant pathway, the initial BOLD response was not significantly affected, but the initial decline was reduced, leading to significantly higher BOLD signals during nAD compared with the control stimulation group (blue line, Fig. 7A,B). Then, BOLD signals declined and reached similar values as under the control condition. Thus, the positive NMDA receptor modulator also only affected BOLD signals during and immediately after nAD.

3.7. Decline in baseline BOLD signals is not accompanied by an increase in the lactate concentration

Because an elevated lactate concentration would indicate a hypoxic state during the period of sustained reduced baseline BOLD signals, we used ¹H NMR spectroscopy to measure the lactate concentration before and after the induction of nAD. Stimulation of the right perforant pathway with a high-intensity pulse sequence elicited similar changes in BOLD baseline signals in the right and left hippocampus. We therefore used the left hippocampus for the measurement because the electrodes did not cause susceptibility artifacts.

In a first set of experiments, we performed two consecutive identical ¹H NMR measurements—one before and one after the stimulation

period (Fig. 8A). Although stimulation induced nAD, the amount of lactate as a marker for increased glycolysis remained unaffected (before: $0.36 \pm 0.40 \ \mu mol/g$, after: $0.73 \pm 0.40 \ \mu mol/g$, p = 0.14; or relative to total creatine [tCr, set at 1.0] before: 0.05 ± 0.05 and after 0.1 ± 0.05 , p = 0.12; Fig. 8A, Table S1). Given the variability of lactate concentration in the unstimulated state, lactate concentration would have had to increase to more than 1 $\mu mol/g$ after stimulation to become significant.

As mentioned before (Fig. S1), repetitive stimulations of the right perforant pathway with high-intensity pulse bursts triggered a decline in baseline BOLD signals as well as transient positive BOLD responses in the left hippocampus. To test whether during repetitive neuronal activation the lactate concentration increases, we again used the left hippocampus for 1 H NMR spectroscopy. Under the condition of repetitive stimulations with high-frequency pulse bursts, there was again no significant increase in lactate (before: $0.28 \pm 0.29 \, \mu \text{mol/g}$, after: $0.84 \pm 0.86 \, \mu \text{mol/g}$, p = 0.13; or relative to tCr [set at 1.0] before: 0.03 ± 0.03 and after 0.1 ± 0.1 , p = 0.12; Fig. 8B, Table S2).

3.8. Susceptibility to subsequent nAD

To check whether the altered hemodynamics affected the susceptibility to subsequent nAD, we performed the same experiment again and

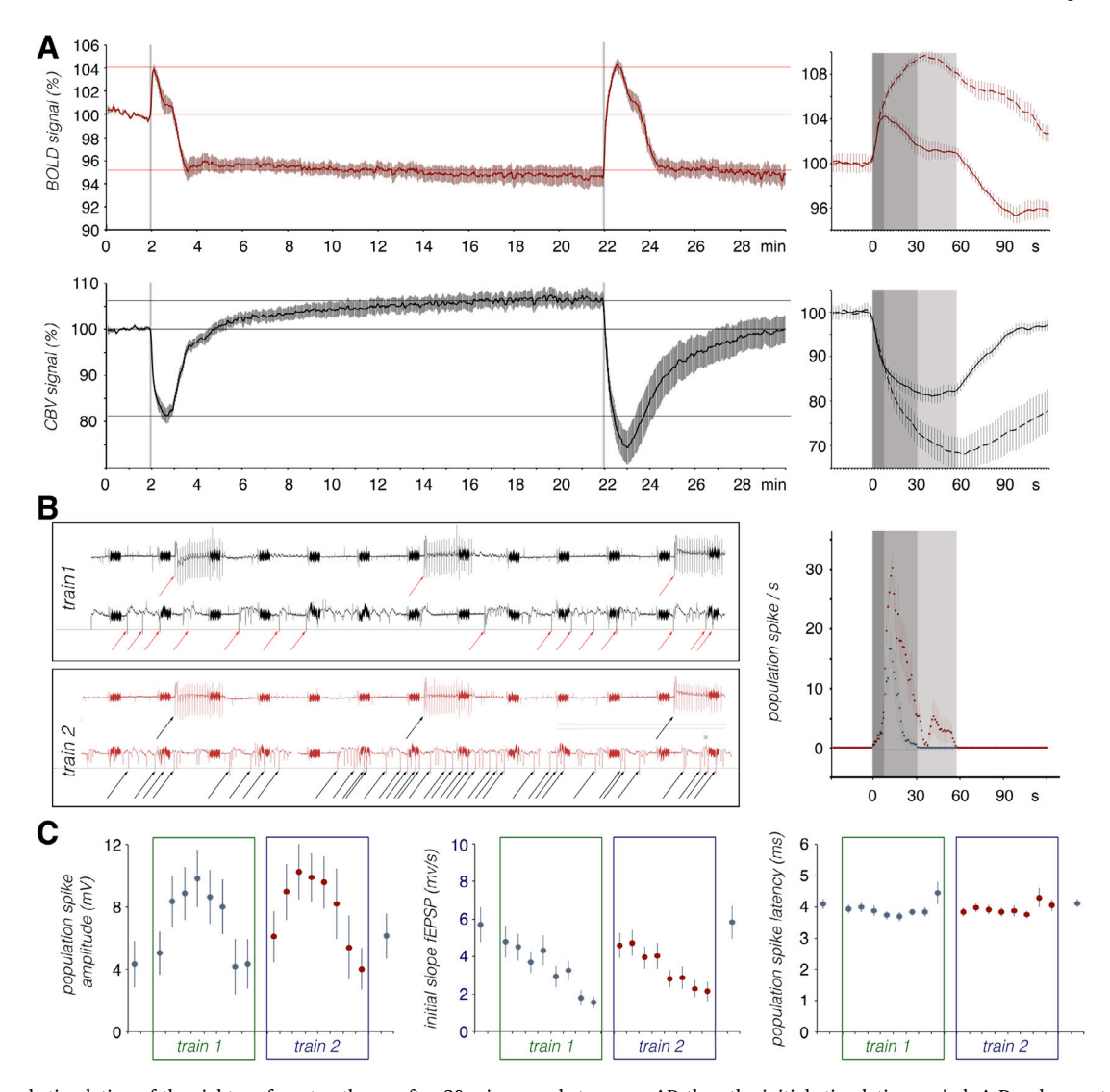


Fig. 9. A second stimulation of the right perforant pathway after 20 min caused stronger nAD than the initial stimulation period. A Development of BOLD (top) and CBV (bottom) signals during the experiment. After baseline BOLD signals declined following the first stimulation period, the second stimulation period caused an increase in BOLD signals to the same level as during the first stimulation period. Right side: comparison of fMRI responses to the first (solid lines) and second (dashed lines) stimulation periods. B Examples of field potential recordings during the period of stimulation (upper row) and subsequent period of h-nAD (lower row) measured during the first (top box) and second (lower box) stimulation trains. Arrows indicate the positions of population spikes. Right side: summary of measured population spikes per second during the first (black dots) and second (red dots) stimulation periods. C Summary of neuronal responses recorded in the dentate gyrus during the first (black dots) and second (red dots) stimulation periods, similar neuronal responses were observed (For interpretation of the references to color in this figure legend, the reader is referred to the web version of this article.).

stimulated the right perforant pathway a second time 20 min after the first stimulation, at a time when baseline BOLD signals were still reduced in the hippocampus and ongoing neuronal activity had apparently normalized. Stimulation at this late time point triggered similar neuronal responses to individual pulse bursts compared with the first stimulation period, but significantly longer and stronger nAD (Fig. 9B,C). Thus, the first stimulation period elicited nAD that lasted 17.8 \pm 9.3 s (the first 7.8 \pm 4.5 s with strong spiking activity), whereas the second stimulation period triggered nAD that lasted 44.0 \pm 13.9 s (the first 30.4 \pm 14.3 s with strong spiking activity). Furthermore, nAD after the second stimulation period were also characterized by more frequent spiking (Fig. 9B). Thus, 20 min after the first stimulation period the susceptibility to generate nAD was increased.

In agreement with the electrophysiological data, the corresponding BOLD responses also differed between the first and second stimulation trains. While the initial rising slopes were similar during the two stimulation trains, the BOLD signals varied during the subsequent nAD period;

they dropped after the first train but continued to rise during the second nAD period. Thus, the second stimulation train caused a stronger and longer positive BOLD response at the end than after the first stimulation train. However, the baseline BOLD signals did not decrease further after the second stimulation period. Comparing the first with the second BOLD response, it is clear that the stronger second BOLD response is mainly related to the difference in the respective BOLD baseline present, because the maximum BOLD signal intensity reached during the two stimulation periods was almost identical (red lines, Fig. 9A). Similarly to the BOLD responses, the two successive stimulation periods produced different CBV responses; however, during the second stimulation period, the maximum CBV signals even exceeded those of the first, so the difference was not only due to a different baseline (black lines Fig. 9A).

When the same stimulation train was repeated continuously with only 1-min intervals, then an identical train after 20 min only caused a smaller BOLD response as the initial response and no nAD. In contrast to the reduced BOLD response in the right dentate gyrus, concurrently

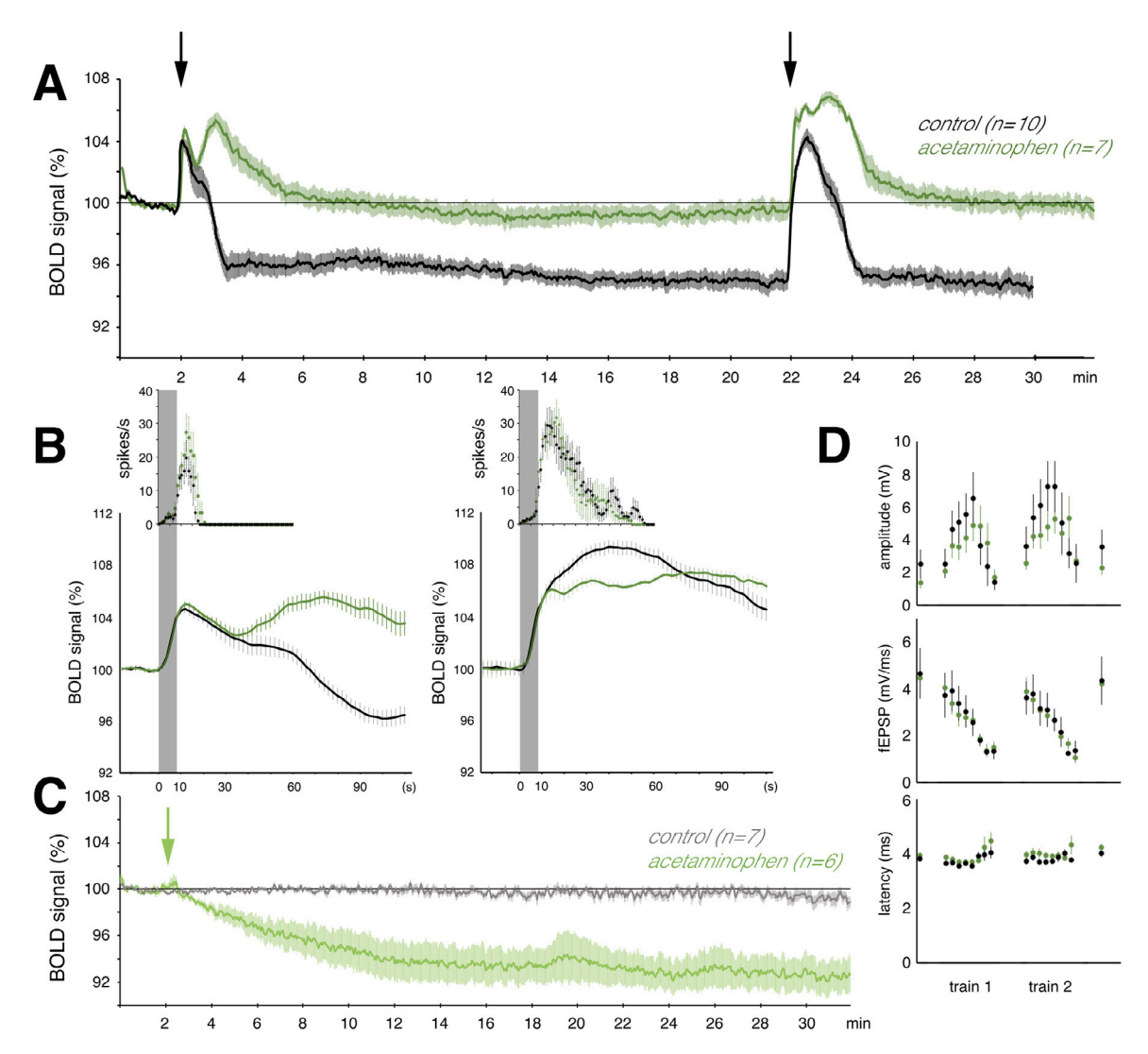


Fig. 10. The presence of acetaminophen only apparently prevents a baseline BOLD signal decline after nAD. A When acetaminophen was applied 30 min before the first stimulation, stimulus-induced nAD caused no significant change in baseline BOLD signals (green line). By contrast, when no acetaminophen was present, baseline BOLD signals declined after the first stimulation period (black line) and remained at this level after the second stimulation period. Black arrows indicate onset of stimulation. B Summary of neuronal and hemodynamic responses during the first (left side) and second (right side) stimulation periods. The duration and strength of nAD elicited during the first and second stimulation periods were not affected by acetaminophen (acetaminophen-treated animals: green dots; untreated animals: black dots). The initial BOLD response was also the same in the two groups. However, in the subsequent course, the BOLD responses differed. During the first stimulation period, the BOLD signals increased a second time before returning only to baseline. After the second stimulation period, the maximum BOLD response was lower in the acetaminophen-treated group. C Intraperitoneal application of acetaminophen (indicated by the green arrow) caused a decline in baseline BOLD signals in the dentate gyrus. Thus, 30 min after application, baseline BOLD signals were at a level as seen after nAD in control animals. D Neuronal responses to individual pulse bursts during the first and second stimulation period were similar in untreated (black dots) and acetaminophen-treated (green dots) animals (For interpretation of the references to color in this figure legend, the reader is referred to the web version of this article.).

elicited neuronal responses were similar. Thus, repetitive stimulations prevented the re-appearance of nAD (Fig. S5). Again, baseline BOLD signals only declined after the initially induced nAD and developed in the presence of repetitive stimulations in a similar way as they did after only one period of nAD.

3.9. Acetaminophen prevented the decline in the baseline BOLD signal

Previous work showed that acetaminophen can prevent postictal hypoperfusion/hypoxia in the mouse hippocampus (Farrell et al., 2016, 2020). We therefore tested whether acetaminophen also affects the nAD-induced decrease in baseline BOLD signals (Fig. 10).

When 250 mg/kg $_{\rm body\ weight}$ acetaminophen was applied 30 min before the onset of stimulation, neither pulse-induced neuronal responses

nor nAD changed, so the neuronal activation pattern was unchanged in the presence of acetaminophen (Fig. 10B,D). BOLD signals during the first and second stimulation period developed similarly compared with untreated animals, but after the first stimulation period, BOLD signals increased a second time during phase 3, the time period when in control animals BOLD signals declined to a significantly lower level. Then BOLD signals only declined to the initial level and remained at this level for at least 20 min. Thus, in the presence of acetaminophen nAD did not cause a decline in baseline BOLD signals (Fig. 10A). In the presence of acetaminophen, a second identical stimulation after 20 min also caused significantly longer and stronger nAD, as observed in the control condition. Thus, the elicitation of stronger nAD during the second stimulation period did not depend on a previous decrease in baseline BOLD signals; it was caused solely by the previous stimulation. Again, stimulus-related BOLD signal changes matched the BOLD responses in control animals,

but the subsequent increase was not as strong as during the control condition.

In an associated experiment, we also checked whether acetaminophen alone affects the development of baseline BOLD signals. After injection of acetaminophen, baseline BOLD signals declined significantly during the next 10 min and remained at this low level for the following 20 min (Fig. 10C). In other words, when the perforant pathway was electrically stimulated 30 min after acetaminophen application, baseline BOLD signals were already at a low level.

4. Discussion

In the current study, we stimulated the right perforant pathway for a short period with eight high-frequency pulse bursts to evoke with high incidence nAD in the hippocampus, which lasted approximately 20 s. The initial pulse-induced neuronal activity elicited a significant positive BOLD response with a corresponding increase in CBV, consistent with an expected functional hyperemia. However, subsequent nAD caused a strong (i.e., more than 5%) and long-lasting (i.e., more than 30 min) decrease in baseline BOLD signals as well as CBV in the hippocampus, corresponding to a long-lasting functional hypoperfusion. The nADinduced decrease in baseline BOLD signals was not prevented by MK801, an NMDA receptor antagonist, nor was it associated with signs of hypoxic metabolism. Furthermore, ongoing neuronal activity in the dentate gyrus that were disturbed by nAD recovered within 20 min; thus, the long-lasting change in baseline BOLD signals did not reflect concurrent changes in ongoing neuronal activity. Pulse-induced neuronal activity in the dentate gyrus also remained unchanged after baseline BOLD was decreased. Thus, all the observed results rule out that the decline in baseline BOLD signals reflects spreading depression (Ayata and Lauritzen, 2015; Busija et al., 2007; Mathias et al., 2018) caused by nAD. Once the baseline BOLD signals stabilized at the lower level, subsequent nAD did not change baseline BOLD signals any further. Similarly, nAD also did not cause a baseline BOLD shift when acetaminophen was already given before stimulation. However, this phenomenon was due to the fact that acetaminophen alone already reduced baseline BOLD signals to the same extent that they were reduced under control conditions by the first nAD. A limitation of this study arises from the distortions in the EPI-fMR images caused by the electrodes, which interfere with a reliable assignment of the fMRI signals generated only in the dentate gyrus. However, in all other subregions of the dorsal hippocampus, BOLD and CBV values developed similarly to those in the dentate gyrus, so that possible confounding volume effects remained rather negligible.

The results suggest that there are at least two relatively stable states of blood supply in the hippocampus, one with a high blood supply and one with a lower blood supply, with both states ensuring apparently normal neuronal functions. Both nAD and acetaminophen are capable of switching the blood supply from a stable high to a stable low state, whereas the conditions that cause the opposite are still unknown. The functional relevance and consequence of the presence of two distinct stable blood supply states remains to be elucidated, but conceptually it suggests that certain short-term neuronal activity has long-lasting effects on the vasculature. Moreover, this activity is not directly related to subsequent neuronal activity. This, in turn, accounts for the fact that an identical stimulus can produce different hemodynamic responses even though it triggers similar neuronal activity.

4.1. How do BOLD and CBV signals follow neuronal activity?

There is a general assumption that a local increase in neuronal activity causes functional hyperemia: A resulting increase in local blood volume (as a result of increased blood flow) leads to greater capillary and venous blood oxygenation (and in turn increases BOLD signals), because more oxygen is supplied than actually consumed (Attwell et al., 2010). By contrast, there is no accepted general mechanism for a

stimulus-related decline in BOLD signals. So far, the assumed mechanisms are increased (mainly inhibitory) activity that is not supported by a concurrent increased blood flow as well as a "blood steal" phenomenon (Bressler et al., 2007; Harel et al., 2002; Pasley et al., 2007; Schridde et al., 2008; Shmuel et al., 2006). In the current study, after the first high-frequency pulse burst stimulation, we observed a transient positive followed by a sustained negative BOLD signal change in the hippocampus. This phenomenon is consistent with the observation that the stimulus also produced two distinguishable forms of neuronal activity, initially a synchronized, coordinated response to each individual electrical impulse and then, with a short delay, nAD. We measured stimulusinduced neuronal activity during two different fMRI experiments, once in the absence of USPIO (BOLD signals) and once in the presence of USPIO (CBV signals). We used an identical measurement sequence for the two fMRI measurements, and thus the spatial and temporal resolution for imaging these two different hemodynamic parameters is also

Because the stimulation protocol did not always trigger nAD, we could estimate BOLD and CBV signal changes caused by the initial, electrical-pulse-triggered neuronal activity as well as the subsequent nAD-triggered neuronal activity (Fig. 4). In all animals, initial BOLD signals increased rapidly and reached the maximum value after 10 s in animals. Thus, it should represent the BOLD response to pulse-related neuronal activity, that is, eight population spikes (one per burst or second) and up to 160 fEPSPs. Thereafter, BOLD signals declined rapidly to the initial baseline in the absence of nAD or decreased only slowly in the presence of nAD; in other words, BOLD signals decreased even in the presence of significantly enhanced spiking activity (see Figs. 2C and 5). Thus, during nAD the BOLD signals did not obviously follow granule cell activity.

In contrast to the BOLD signals, the changes in CBV signals were more closely related to the measured parameters of granule cell activity. In particular, during nAD—the period with the strongest spiking activity—CBV also continued to increase. Because BOLD signals represent a complex hemodynamic parameter that depends on both CBV (controlled by cerebral blood flow) and tissue oxygen consumption (CMRO2), changes in CMRO2 can be roughly estimated from the two measured signals: $BOLD_{signal} = -CBV_{signal} - CMRO_2$. Of note, the CBV signal develops inversely to the actual CBV because the presence of USPIO used to measure CBV reduces the MRI signal. The equation can be rearranged to: $CMRO_2 = -CBV_{signal} - BOLD_{signal}$. According to that, CMRO₂ strongly increased during the period of nAD and even further during and after termination of nAD (Figs. 5 and 6). Thus, the period in which nAD are terminated is characterized by the highest oxygen consumption, indicating that nAD termination is an active process rather than the result of simple neuronal exhaustion.

The fact that energy depletion is not the main reason why termination of nAD is also supported by the observation that an identical stimulation 1 min later, at a time point when CMRO2 was still at the highest level, resulted in a similar pulse-related spiking and postsynaptic activity (Fig. S5). However, population spike latencies were significantly increased, indicating the presence of an additional inhibitory process that was not active during the initial stimulation period. Similarly to the population spike latency, CMRO₂ returned to the initial level during the subsequent 2 min. Thus, we assume that the high oxygen consumption at the end of nAD and especially after their termination represents a highly active inhibitory mechanism that successfully counteracted the seizure-like activity. According to the development of CMRO2, the activity of this inhibitory mechanism ceased after about 3-4 min. This agrees with previous observations that nAD were not induced when an identical stimulation was applied 2 min later (Helbing et al., 2017), but were generated when the interval was extended to 5 min (Angenstein, 2019). Based on this, we conclude that during nAD, inhibitory mechanisms became transiently active and effectively suppressed seizure-like neuronal activity. This highly oxygen-consuming (i.e., energy demanding) mechanism lasting for a short time (i.e., longer than 2 but less than 5 min)

and could therefore not be responsible for the sustained decline in baseline BOLD signals. In fact, only 3–4 min after termination of nAD, CBV declined below the initial level, at a time point when nAD-induced inhibitory activity had vanished. In addition, during the period where reduced CBV was observed, tissue oxygen consumption returned to baseline levels, suggesting that total neuronal activity returned to a level similar to that before the onset of electrical stimulation. This finding is also consistent with field recordings in the dentate gyrus (Fig. 6). Thus, another mechanism has to be responsible for the sustained decline in CBV and by it the sustained decline in baseline BOLD signals. Conceptually, two basic mechanisms are conceivable: first, long-term activation of a vasoconstrictor mechanism (i.e., an active mechanism), and, second, loss of a previously permanently active vasodilator mechanism (i.e., a passive mechanism).

On the basis of the presented results, we hypothesize that the sustained decrease in CBV after nAD reflects an inhibition of a previously active vasodilatory mechanism rather than a sustained vasoconstriction: (i) nAD-induced decline in baseline BOLD signals persisted for at least 2 h. The decline was still occasionally interrupted by spontaneous positive BOLD waves (Fig. S3), so the presence of permanent vasoconstriction is unlikely, as previously observed after induction of tonic-clonic seizures in mice (Tran et al., 2020). (ii) Neurovascular coupling mechanisms remained intact after the decline in baseline BOLD signals. Whether acetaminophen or nAD caused a baseline BOLD shift, subsequent stimulation still produced positive hemodynamic responses (Figs. 9, 10 and S5). (iii) nAD did not induce a persistent change in tissue oxygen consumption (Fig. 6) or changes in lactate concentration (Fig. 8). Thus, there is no metabolic marker for a sustained increased neuronal activity that maintains vasoconstriction. (iv) nAD only triggered a transient change in the quantity of ongoing neuronal activity. After termination of nAD, overall neuronal activity almost completely disappeared, but within 6 min it had already returned to a level similar to that before the start of stimulation. That is, there is also no electrophysiological evidence of continuous increased neuronal activity that could have a lasting effect on the vasculature. (v) The decrease in BOLD signals occurred despite increased neuronal activity. The decrease in BOLD signals below baseline occurred mainly during the period of secondary nAD (phase 4, Fig. 5), i.e., during a period of markedly increased neuronal activity. However, when acetaminophen was administered before stimulation, thus already causing a decrease in baseline BOLD signals, the same period of secondary nAD resulted in a marked increase in BOLD signals. This suggests that under control conditions at this time, the existing continuous vasodilatory activity disappeared, masking normal functional hyperemia.

The assumption that nAD terminates an ongoing constitutively active vasodilatation supports previous findings suggesting that astrocytes provide constant vasodilation through a constitutive release of prostaglandins via continuous COX-1 activity (Rosenegger et al., 2015). In addition, hippocampal (excitatory) neurons are known to constitutively express COX-2; thus, an additional source for the generation of vasodilatory compounds may exist (Kaufmann et al., 1996; López and Ballaz, 2020; Pepicelli et al., 2005; Yamagata et al., 1993). Neuronalactivity-dependent inhibition of COX enzymes has not yet been described, whereas increased expression of COX-2 has been shown to persist for at least 8 h after the onset of a spreading depression or epileptic seizures (Takemiya et al., 2006). Whether the increased expression of COX-2 is the result of prior enzyme inhibition is unclear. The fact that acetaminophen and nAD caused a similar shift in baseline BOLD signals and both treatments were not additive (i.e., nAD did not alter baseline BOLD signals 30 min after acetaminophen administration) suggests that both treatments may affect a common mechanism, in particular COX-1/2-metabolite-mediated effects. In addition, acetaminophen is known to activate cannabinoid CB1 and CB2 receptors as well as TRPV1 channels via its metabolite AM404, which is thought to mediate the analgesic effect of this drug (Ohashi and Kohno, 2020). However, it is unlikely that activation of these pathways was mainly responsible for the sustained decrease in BOLD signaling in our experiments, because activation of CB1 tends to increase BOLD signals in rats (Shah et al., 2004), and TRPV channels are poorly expressed in the rat hippocampus (Cavanaugh et al., 2011)

All experiments were performed in the presence of the sedative medetomidine to avoid motion artifacts that would likely occur during the long scan time. However, medetomidine, as a noradrenergic alpha2 agonist, also modifies central adrenergic functions and may cause vasoconstriction by directly binding to corresponding receptors on brain vessels, thereby itself causing a reduction in CBV (Jonckers et al., 2015; Pawela et al., 2009; Weber et al., 2006). This effect depends on the dose and delivery method—for example, topical versus systemic (Jonckers et al., 2015). We cannot rule out such a confounding effect of medetomidine on the observed long-lasting, stimulus-induced baseline BOLD shift, in particular during later time points, that is, after 40 min when a decline in baseline BOLD signals occurred in the hippocampus even under unstimulated conditions (Fig. 2D). In fact, it was also observed that an approximately 5% decrease in BOLD signals was caused by medetomidine after 30 min when the same bolus injection of medetomidine was followed by a continuous i.v. injection of 0.3 mg/kg body weight/h medetomidine. This effect was not detectable with continuous i.v. administration of 0.1 mg/kg body weight /h medetomidine (Abe et al., 2017). However, in our study using 0.1 mg/kg body weight /h medetomidine, only in the regions directly activated by the hippocampus (i.e., septum and mPFC) was there an additional decrease in BOLD signals compared with the unstimulated animals, whereas in the regions not directly affected by hippocampal efferents (i.e., right dorsal striatum and cerebellum), BOLD signals declined similarly to those in the unstimulated animals after a single stimulation of the perforant pathway (Fig. S6). Thus, the stimulus-induced decrease in baseline BOLD signals added to the medetomidine-induced decrease in baseline BOLD signals. To minimize this confounding effect of medetomidine on overall hemodynamics, we considered only a period up to 30 min after the initial stimulation phase in the current study. This does not rule out the possibility that medetomidine had no prior effects on general hemodynamics, as previously described (Sirmpilatze et al., 2019). According to this study, medetomidine induces a transitional state that stabilizes after approximately 30 min. This time point also corresponds to the start of our fMRI experiments and would also explain why the BOLD signals remained constant for at least 40 min under control conditions.

4.2. Sustained decline in baseline BOLD signals as a biomarker for a postictal period?

A short electrical high-frequency pulse burst stimulation of the perforant pathway elicited nAD, similarly to epileptic discharges. All nAD episodes were followed by a period of almost complete loss of ongoing activity before a second period of higher neuronal activity. In particular, during the second brief period of increased neuronal activity, BOLD signals decreased and did not recover thereafter, although overall ongoing neuronal activity appeared to normalize. The decrease in BOLD signals occurred only after triggering nAD and was not observed when the same stimulation did not elicit nAD. Identical stimulation 20 min later caused significantly stronger nAD, that is, local neuronal network properties must have been altered in a long-lasting manner during the first stimulation period. This is partly consistent with the observation that after nAD the power of individual frequency bands also changed. Thus, ongoing theta (4-8 Hz) and slow gamma (30-49 Hz) oscillation did not return to the initial level within 20 min after nAD. This means that many features of a postictal state and the observed drop in the baseline BOLD signals coincide, namely triggering by seizure-like neuronal activity, a long duration, and the presence of long-lasting altered neuronal circuit properties. Although it is tempting to consider such a baseline BOLD shift as specific marker for the presence/duration of a postictal state, it should be noted that a similar change in baseline BOLD signals was also observed after acetaminophen application alone, that is, in a condition without epileptic discharges. Similarly, a baseline BOLD

signal shift (after acetaminophen application) is not necessarily associated with altered neuronal network properties, as demonstrated by the normal neuronal response during the first electrical stimulation after acetaminophen application. Thus, a long-lasting baseline BOLD drop is not a specific marker for a postictal state; rather, it is a useful, sensitive biomarker to verify the emergence of a postictal state after brief epileptic neuronal activity. Future work, possibly also using this experimental approach, is needed to uncover the cellular mechanisms that may reverse the observed baseline BOLD decline, and then also to test their effect on altered local neuronal network properties. In other words, this experimental approach could be used as a screening system for compounds that shorten the duration of the postictal state.

Declaration of Competing Interest

The author declares no competing financial interests

Credit authorship contribution statement

Alberto Arboit: Conceptualization, Visualization, Data curation, Formal analysis, Writing – review & editing. **Shih-Pi Ku:** Formal analysis, Writing – review & editing. **Karla Krautwald:** Data curation, Formal analysis, Writing – review & editing. **Frank Angenstein:** Conceptualization, Visualization, Data curation, Formal analysis, Writing – original draft, Writing – review & editing.

Acknowledgments

This study was funded by the Deutsche Forschungs-Gemeinschaft (DFG, German Research Foundation) – Project-ID 425899996 – SFB 1436.

Data statement

The data sets generated and/or analyzed during the current study are available upon reasonable request from the corresponding author.

Supplementary materials

Supplementary material associated with this article can be found, in the online version, at doi:10.1016/j.neuroimage.2021.118769.

References

- Abe, Y., Tsurugizawa, T., Le Bihan, D., 2017. Water diffusion closely reveals neural activity status in rat brain loci affected by anesthesia. PLoS Biol. 15, e2001494.
- Angenstein, F., 2019. The role of ongoing neuronal activity for baseline and stimulus-induced BOLD signals in the rat hippocampus. Neuroimage 202, 116082.
- Angenstein, F., Kammerer, E., Niessen, H.G., Frey, J.U., Scheich, H., Frey, S., 2007. Frequency-dependent activation pattern in the rat hippocampus, a simultaneous electrophysiological and fMRI study. Neuroimage 38, 150–163.
- Arboit, A., Krautwald, K., F, A., 2021. The cholinergic system affects negative BOLD responses in the prefrontal cortex that are triggered by neuronal afterdischarges in the hippocampus. J. Cereb. Blood Flow Metab..
- Attwell, D., Buchan, A.M., Charpak, S., Lauritzen, M., Macvicar, B.A., Newman, E.A., 2010.
 Glial and neuronal control of brain blood flow. Nature 468, 232–243.
- Ayata, C., Lauritzen, M., 2015. Spreading depression, spreading depolarizations, and the cerebral vasculature. Physiol. Rev. 95, 953–993.
- Berman, R.F., 2009. Seizures: Seizure Termination and the Postseizure Refractory Period. Encyclopedia of Basic Epilepsy Research, pp. 1320–1327.
- Bovet-Carmona, M., Krautwald, K., Menigoz, A., Vennekens, R., Balschun, D., F, A., 2019. Low frequency pulse stimulation of Schaffer collaterals in Trpm4-/- knockout rats differently affects baseline BOLD signals in target regions of the right hippocampus but not BOLD responses at the site of stimulation. Neuroimage 188, 347–356.
- Bragin, A., Penttonen, M., Buzsaki, G., 1997. Termination of epileptic afterdischarge in the hippocampus. J. Neurosci. 17, 2567–2579.
- Bressler, D., Spotswood, N., Whitney, D., 2007. Negative BOLD fMRI response in the visual cortex carries precise stimulus-specific information. PLoS One 2, e410.
- Busija, D.W., Bari, F., Domoki, F., Louis, T., 2007. Mechanisms involved in the cerebrovascular dilator effects of N-methyl-D-aspartate in cerebral cortex. Brain Res. Rev. 56, 89–100.

Cavanaugh, D.J., Chesler, A.T., Jackson, A.C., Sigal, Y.M., Yamanaka, H., Grant, R., O'Donnell, D., Nicoll, R.A., Shah, N.M., Julius, D., Basbaum, A.I., 2011. Trpv1 reporter mice reveal highly restricted brain distribution and functional expression in arteriolar smooth muscle cells. J. Neurosci. 31, 5067–5077.

- Cohen, M.X., Elger, C.E., Fell, J., 2008. Oscillatory activity and phase-amplitude coupling in the human medial frontal cortex during decision making. J. Cogn. Neurosci. 21, 390–402.
- Farrell, J.S., Colangeli, R., Dudok, B., Wolff, M.D., Nguyen, S.L., Jackson, J., Dickson, C.T., Soltesz, I., Teskey, G.C., 2020. *In vivo* assessment of mechanisms underlying the neurovascular basis of postictal amnesia. Sci. Rep. 10, 14992.
- Farrell, J.S., Gaxiola-Valdez, I., Wolff, M.D., David, L.S., Dika, H.I., Geeraert, B.L., Rachel Wang, X., Singh, S., Spanswick, S.C., Dunn, J.F., Antle, M.C., Federico, P., Teskey, G.C., 2016. Postictal behavioral impairments are due to a severe prolonged hypoperfusion/hypoxia event that is COX-2 dependent. Elife 5.
- Freeman, W.J., 2004. Origin, structure, and role of background EEG activity. Part 1. Analytic amplitude. Clin. Neurophysiol. 115, 2077–2088.
- Harel, N., Lee, S.P., Nagaoka, T., Kim, D.S., Kim, S.G., 2002. Origin of negative blood oxygenation level-dependent fMRI signals. J. Cereb. Blood Flow Metab. 22, 908–917.
- Helbing, C., Tischmeyer, W., Angenstein, F., 2017. Late effect of dopamine D1/5 receptor activation on stimulus-induced BOLD responses in the hippocampus and its target regions depends on the history of previous stimulations. Neuroimage 152, 119–129.
- Helbing, C., Werner, G., Angenstein, F., 2013. Variations in the temporal pattern of perforant pathway stimulation control the activity in the mesolimbic pathway. Neuroimage 64, 43–60.
- Hennig, J., Nauerth, A., Friedburg, H., 1986. RARE imaging: a fast imaging method for clinical MR. Magn. Reson. Med. 3, 823–833.
- Jonckers, E., Shah, D., Hamaide, J., Verhoye, M., Van der Linden, A., 2015. The power of using functional fMRI on small rodents to study brain pharmacology and disease. Front. Pharmacol. 6, 231.
- Kaufmann, W.E., Worley, P.F., Pegg, J., Bremer, M., Isakson, P., 1996. COX-2, a synaptically induced enzyme, is expressed by excitatory neurons at postsynaptic sites in rat cerebral cortex. Proc. Natl. Acad. Sci. U. S. A. 93, 2317–2321.
- Lado, F.A., Moshe, S.L., 2008. How do seizures stop? Epilepsia 49, 1651-1664.
- López, D.E., Ballaz, S.J., 2020. The role of brain cyclooxygenase-2 (Cox-2) beyond neuroinflammation: neuronal homeostasis in memory and anxiety. Mol. Neurobiol. 57, 5167–5176.
- Lu, H., Scholl, C.A., Zuo, Y., Stein, E.A., Yang, Y., 2007. Quantifying the blood oxygenation level dependent effect in cerebral blood volume-weighted functional MRI at 9.4T. Magn. Reson. Med. 58, 616–621.
- Mathias, E.J., Kenny, A., Plank, M.J., David, T., 2018. Integrated models of neurovascular coupling and BOLD signals: responses for varying neural activations. Neuroimage 174, 69–86.
- Ohashi, N., Kohno, T., 2020. Analgesic effect of acetaminophen: a review of known and novel mechanisms of action. Front. Pharmacol. 11, 580289.
- Pasley, B.N., Inglis, B.A., Freeman, R.D., 2007. Analysis of oxygen metabolism implies a neural origin for the negative BOLD response in human visual cortex. Neuroimage 36, 260, 276
- Pawela, C.P., Biswal, B.B., Hudetz, A.G., Schulte, M.L., Li, R., Jones, S.R., Cho, Y.R., Matloub, H.S., Hyde, J.S., 2009. A protocol for use of medetomidine anesthesia in rats for extended studies using task-induced BOLD contrast and resting-state functional connectivity. Neuroimage 46, 1137–1147.
- Pepicelli, O., Fedele, E., Berardi, M., Raiteri, M., Levi, G., Greco, A., Ajmone-Cat, M.A., Minghetti, L., 2005. Cyclo-oxygenase-1 and -2 differently contribute to prostaglandin E2 synthesis and lipid peroxidation after *in vivo* activation of N-methyl-D-aspartate receptors in rat hippocampus. J. Neurochem. 93, 1561–1567.
- Provencher, S.W., 1993. Estimation of metabolite concentrations from localized in vivo proton NMR spectra. Magn. Reson. Med. 30, 672–679.
- Rosenegger, D.G., Tran, C.H., Wamsteeker Cusulin, J.I., Gordon, G.R., 2015. Tonic local brain blood flow control by astrocytes independent of phasic neurovascular coupling. J. Neurosci. 35, 13463–13474.
- Schridde, U., Khubchandani, M., Motelow, J.E., Sanganahalli, B.G., Hyder, F., Blumenfeld, H., 2008. Negative BOLD with large increases in neuronal activity. Cereb. Cortex 18. 1814–1827.
- Shah, Y.B., Prior, M.J., Dixon, A.L., Morris, P.G., Marsden, C.A., 2004. Detection of cannabinoid agonist evoked increase in BOLD contrast in rats using functional magnetic resonance imaging. Neuropharmacology 46, 379–387.
- Shatillo, A., Lipponen, A., Salo, R.A., Tanila, H., Verkhratsky, A., Giniatullin, R., Grohn, O.H., 2019. Spontaneous BOLD waves a novel hemodynamic activity in Sprague-Dawley rat brain detected by functional magnetic resonance imaging. J. Cereb. Blood Flow Metab. 39, 1949–1960.
- Shmuel, A., Augath, M., Oeltermann, A., Logothetis, N.K., 2006. Negative functional MRI response correlates with decreases in neuronal activity in monkey visual area V1. Nat. Neurosci. 9, 569–577.
- Sirmpilatze, N., Baudewig, J., Boretius, S., 2019. Temporal stability of fMRI in medeto-midine-anesthetized rats. Sci. Rep. 9, 16673.
- Takemiya, T., Maehara, M., Matsumura, K., Yasuda, S., Sugiura, H., Yamagata, K., 2006. Prostaglandin E2 produced by late induced COX-2 stimulates hippocampal neuron loss after seizure in the CA3 region. Neurosci. Res. 56, 103–110.
- $\label{eq:charge_equation} Tran, C.H.T., George, A.G., Teskey, G.C., Gordon, G.R., 2020. Seizures elevate gliovascular unit Ca^{2+} and cause sustained vasoconstriction. JCI Insight 5.$
- Weber, R., Ramos-Cabrer, P., Wiedermann, D., van Camp, N., Hoehn, M., 2006. A fully noninvasive and robust experimental protocol for longitudinal fMRI studies in the rat. Neuroimage 29, 1303–1310.
- Yamagata, K., Andreasson, K.I., Kaufmann, W.E., Barnes, C.A., Worley, P.F., 1993. Expression of a mitogen-inducible cyclooxygenase in brain neurons: regulation by synaptic activity and glucocorticoids. Neuron 11, 371–386.